Line shape and strength of two-photon absorption in an atomic vapor with a resonant or nearly resonant intermediate state

J. E. Bjorkholm and P. F. Liao
Bell Laboratories, Holmdel, New Jersey 07733
(Received 5 April 1976)

The line shape and strength of two-photon absorption in an atomic vapor are studied both theoretically and experimentally for the case of absorption of unequal-frequency photons. Special attention is given to the situation in which the intermediate state is resonant or nearly resonant. It is shown that for the resonant case, maximum absorption rates and Doppler-free spectra are *simultaneously* obtained. Either counterpropagating or copropagating beams can be used. With counterpropagating beams the two-photon linewidths are quite insensitive to power broadening of the intermediate state. With copropagating beams the two-photon spectra can also reveal the intermediate-state structure with a resolution determined mainly by the intermediate-state lifetime (nearly as well as can be done using any spectroscopic technique). The theoretical analysis provides a closed-form solution for the line shape and strength of the two-photon spectrum. In general the line shape is composed of two features. One is Doppler broadened and predominates when the intermediate state is nonresonant. The second feature is Doppler free, and it predominates with a resonant intermediate state. Detailed comparisons of experimental measurements of the line shape and strength of two-photon absorption in Na vapor are made with the theory and found to be in excellent agreement. Signal strengths for the on-resonance case are 6×10^9 larger than the case of equal-frequency photons with no loss in resolution.

I. INTRODUCTION

There has been a great deal of recent interest in Doppler-free two-photon spectroscopy carried out in atomic or molecular vapors by using *equal*-frequency laser beams, propagating in opposite directions through the sample, to induce the two-photon absorption.[1] In these experiments Doppler broadening is eliminated because the first-order Doppler shift of the frequencies of the two laser beams seen by a moving observer are of equal magnitude and of opposite sign. Thus the sum frequency is independent of velocity. In some situations, however, it is advantageous to use *unequal*-frequency photons[2]; for instance, it has been shown that the two-photon absorption rate (and hence the signal strength) usually can be increased many orders of magnitude by making use of resonant enhancement with an intermediate state.[3] With oppositely propagating unequal-frequency laser beams, however, Doppler effects are normally not fully eliminated to first order and residual Doppler broadening is present.

In this paper we theoretically and experimentally consider the situation which results when one of the laser frequencies is tuned to be resonant, or nearly resonant, with the ground-to-intermediate-state transition frequency. In particular, we have studied the line shape and strength of the two-photon spectrum as a function of the degree of mistuning of the lasers from exact intermediate-state resonance. We shall refer to the situation of exact resonance as the on-resonance case.

The most important findings are as follows: First, we demonstrate that maximum absorption rates and Doppler-free spectra are *simultaneously* obtained for the on-resonance case; either counterpropagating or copropagating laser beams can be used. Secondly, for the on-resonance case, the two-photon spectra yield information about the structure of the ground, intermediate, and final states; by contrast, for the off-resonance case, such information about the intermediate state is not obtained. These facts are not widely appreciated, even though they are implicit in earlier treatments of "laser-induced line narrowing."[4,5] Our analysis provides a closed-form solution for the line shape and strength of the two-photon spectrum and is in good agreement with the experimental measurements reported here. The strength of the Doppler-free spectrum obtained for the on-resonance case is about 6×10^9 larger than that obtained using oppositely propagating equal-frequency laser beams.

In Sec. II we present a theory for the two-photon transition rate in a vapor for arbitrary mistuning of the lasers from resonance with the intermediate state. For clarity and simplicity we restrict our consideration to low optical intensities and no collisions. Calculations of a similar nature are being carried out for the more complicated case which includes collisions and arbitrary light intensities by Salomaa and Stenholm.[6,7]

We consider the situation shown in Fig. 1. Laser beams having frequencies ν_1 and ν_2 interact with a three-level atom having a ground state g of energy E_g, an intermediate state i of energy E_i, and a final state f of energy E_f. Transitions be-

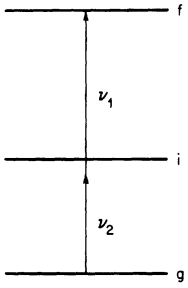

FIG. 1. Energy levels of a simplified three-level atom interacting with light at the frequencies ν_1 and ν_2.

tween the states g and i and between the states i and f are electric dipole allowed. The single-photon transition frequencies are $\nu_{ig}=(E_i-E_g)/h$ and $\nu_{fi}=(E_f-E_i)/h$. The two-photon transition frequency is $\nu_{fg}=(E_f-E_g)/h$. We find that the generalized two-photon spectrum is composed of two types of lines. The first type[8] predominates for the off-resonance case when both $|\nu_1-\nu_{ig}|$ and $|\nu_2-\nu_{ig}|$ are large compared with the Doppler width $\Delta_{ig}=(8kT\ln 2/m)^{1/2}\nu_{ig}/c$ of the single-photon $g\rightarrow i$ transition. This two-photon line occurs when $\nu_1+\nu_2=\nu_{fg}$ (aside from frequency-pulling effects to be described later), it has a line shape described by the Voigt profile (a Gaussian convolved with a Lorentzian), and it has a Doppler-broadened linewidth [full width at half-maximum (FWHM)] given approximately by

$$|(\nu_2+\epsilon\nu_1)/\nu_{fg}|\,\Delta_{fg}=|(\nu_2+\epsilon\nu_1)/\nu_{ig}|\,\Delta_{ig} \qquad (1.1)$$

when the linewidth is large compared to the natural width of the final state. In the above, Δ_{fg} is the usual Doppler width of the two-photon transition and the parameter ϵ equals $+1$ or -1 depending upon whether the laser beams are copropagating or counterpropagating, respectively. The second type of spectral line predominates for the on-resonance case, $|\nu_2-\nu_{ig}|<\Delta_{ig}$, and it is free of Doppler broadening. The line shape is Lorentzian and its linewidth (FWHM) is given by

$$\Delta\nu_f+|(\nu_2+\epsilon\nu_1)/\nu_{ig}|\,\Delta\nu_i\,, \qquad (1.2)$$

where $\Delta\nu_f$ and $\Delta\nu_i$ are the natural linewidths of the final and intermediate states, respectively. The exact sum frequency, $\nu_1+\nu_2$, at which this line appears depends upon ν_2, although, of course, $\nu_1+\nu_2\approx\nu_{fg}$. When $|\nu_2-\nu_{ig}|\approx\Delta_{ig}$ the two types of lines are of comparable magnitude and the two-photon line shape is a more complicated combination of the two types of lines.

A qualitative understanding of the line narrowing which results for the on-resonance situation is obtained using a simple "hole-burning" argument.[9] The light at ν_2 is resonant with a particular velocity group of atoms for the $g\rightarrow i$ transition. This group is composed of those atoms whose velocities are such that $|\nu_{ig}-(1-v/c)\nu_2|\leq\Delta\nu_i$. The two-photon transition rate for these atoms is greatly enhanced over that for all other velocity groups, so that the spectrum is essentially due to only the resonant velocity group. In effect, we have narrowed the velocity distribution, so that Δ_{ig} in Eq. (1.1) should be replaced with $\Delta\nu_i$, with the result that the total linewidth (also accounting for the natural linewidth of the final state) is that given in Eq. (1.2) and is Doppler free.

Two-photon absorption with a resonant intermediate state, the on-resonance case, is often treated as an interaction distinct from the off-resonance case. It has often been referred to as two-step or stepwise absorption. Our analysis shows that at least for the collisionless case there is no need to make a distinction between the two types of transitions. We treat them both in a unified fashion and refer to both cases as two-photon absorption.

In Sec. III we describe our experiments, which are extensions of work on which we have previously reported.[3] In some respects our experiments are also similar to a recently reported experiment in which laser-induced absorption line narrowing was observed.[10] Basically, we use two continuously tunable single-mode cw dye lasers operating at different frequencies to induce two-photon transitions in sodium vapor. The transitions take place between the $3S$ ground state and the $4D$ excited state; either the $3P_{3/2}$ or $3P_{1/2}$ level was used as the predominant intermediate state. Spectra were obtained by keeping the frequency ν_2 of one laser fixed while scanning the frequency ν_1 of the other laser. The experimentally observed dependence of the line shape and line strength upon $|\nu_2-\nu_{ig}|$ is shown to be in good agreement with the theory derived in Sec. II. We also demonstrate that when copropagating beams are used for the on-resonance case, the spectroscopy of the intermediate state can also be obtained. The various hyperfine components of the intermediate state give spectral components at frequencies separated by ν_{fg}/ν_{ig} times the hyperfine splitting. Thus if $\Delta\nu_f\ll\Delta\nu_i$ Eq. (1.2) shows that it is possible to obtain spectra of the intermediate state with a resolution limited by $\Delta\nu_i$ and comparable to that obtained with other Doppler-free spectroscopic techniques, such as saturation spectroscopy or single-photon excitation of an atomic beam.

II. THEORY

Although much of the theory of coupled three-level systems has been discussed previously,[4] for

completeness we outline a calculation of the line shape and strength of two-photon absorption for the simple three-level atom diagrammed in Fig. 1. In our experiment, and in most two-photon experiments to date, the two-photon transition rate is monitored by observing the fluorescence which results when atoms decay from the excited state. Thus we calculate the probability that the excited state f is populated. Our analysis considers steady-state excitation and uses standard time-dependent perturbation theory.

We start by calculating the steady-state two-photon transition rate for a stationary atom. The atom is illuminated by two optical beams at the frequencies $\omega_1 = 2\pi\nu_1$ and $\omega_2 = 2\pi\nu_2$ which propagate along the z axis. The optical electric fields are given as

$$\vec{\mathcal{E}}_1(z,t) = \vec{\mathcal{E}}_{10}\cos(\omega_1 t - \epsilon k_1 z),$$
$$\vec{\mathcal{E}}_2(z,t) = \vec{\mathcal{E}}_{20}\cos(\omega_2 t - k_2 z).$$

The parameter ϵ specifies the relative propagation directions of the laser beams; for co-propagating beams we have $\epsilon = +1$ and for oppositely propagating beams we have $\epsilon = -1$.

The atomic wave function $\psi(t)$ satisfies the time-dependent Schrödinger equation which we solve using standard second-order perturbation theory. We expand $\psi(t)$ in terms of the time-independent eigenfunctions $\psi_k^{(0)}$ of the unperturbed atom, which have eigenenergies $E_k^{(0)}$. Thus

$$\psi(t) = \sum_k a_k(t)\psi_k^{(0)} e^{-i(E_k/\hbar)t}, \tag{2.1}$$

where the $a_k(t)$ are the time-dependent probability amplitudes for finding the atom in state k. With this substitution the time-dependent Schrödinger equation becomes

$$i\hbar\dot{a}_m = -\frac{i\hbar}{2\tau_m}a_m + \sum_k a_k V_{mk}(t)e^{i\omega_{mk}t}, \tag{2.2}$$

where we have phenomenologically accounted for damping of the atomic system by introducing τ_k, the natural lifetime of the kth energy level. Also, we have used $\hbar\omega_{mk} = E_m^{(0)} - E_k^{(0)}$ and

$$V_{mk}(t) = \langle\psi_m^{(0)}|\, V(t)\,|\,\psi_k^{(0)}\rangle, \tag{2.3}$$

where $V(t)$ is that part of the total Hamiltonian which describes the interaction of the applied optical field with the atom. In the electric dipole approximation and for linearly polarized optical electric fields we have $V(t) = -\vec{p}\cdot\vec{\mathcal{E}}(t)$, where $\vec{p}$ is the dipole moment operator for the atom.

We are now prepared to solve Eq. (2.3) for the steady-state solution of $a_f(t)$. For simplicity we restrict our attention to low optical field strengths, so that saturation and ac Stark effects are avoided, and hence $|a_g(t)| \simeq 1$, $|a_i(t)| \ll 1$, and $|a_f(t)| \ll 1$. The method of solution is as follows: First we use the rotating-wave approximation to solve Eq. (2.2) for the steady-state solution $a_i^{(1)}(t)$ with the assumption that $a_g^{(1)}(t) = 1$ and $a_f^{(1)}(t) = 0$. This solution for $a_i^{(1)}(t)$ is then reinserted into Eq. (2.3) to solve for $a_f^{(2)}(t)$. In order to maintain simplicity and ease of physical interpretation we further assume that ν_{ig} and ν_{fi} are considerably different; in particular we require $|\nu_{ig} - \nu_{fi}| \gg \Delta_{ig}$. We further assume that $\nu_2 \approx \nu_{ig}$ and $\nu_1 \approx \nu_{fi}$ such that $|\nu_2 - \nu_{ig}| \ll |\nu_1 - \nu_{ig}|$ and $|\nu_1 - \nu_{fi}| \ll |\nu_2 - \nu_{fi}|$. In this way we assure that light at ν_2 is much more effective in producing $g \to i$ transitions than is light at ν_1. Similarly, light at ν_1 is much more effective than light at ν_2 in inducing $i \to f$ transitions. This restriction is not a severe one and, in fact, is usually satisfied in most atoms or molecules for nearly resonant intermediate states. It is well satisfied in our experiments. Extension to the more general case is straightforward.

With the aforementioned assumptions we find the desired result to be

$$|a_f^{(2)}|^2 = \frac{|\beta_1|^2\,|\beta_2|^2}{(\Omega_2^2 + 1/4\tau_i^2)[(\Omega_1+\Omega_2)^2 + 1/4\tau_f^2]}, \tag{2.4}$$

where we have introduced the parameters $\Omega_2 = \omega_2 - \omega_{ig}$, $\Omega_1 = \omega_1 - \omega_{fi}$, $\beta_2 = \vec{p}_{ig}\cdot\vec{\mathcal{E}}_{20}/2\hbar$, and $\beta_1 = \vec{p}_{fi}\cdot\vec{\mathcal{E}}_{10}/2\hbar$. The quantity $\vec{p}_{mn}$ is the dipole matrix element between states m and n. The steady-state two-photon transition rate for the stationary atom is simply $\Gamma = |a_f^{(2)}|^2/\tau_f$. From Eq. (2.4) it is clear that Γ has two resonant denominators. The first resonance occurs for $\Omega_1 + \Omega_2 = \omega_1 + \omega_2 - \omega_{fg} = 0$ and is the two-photon resonance. The other resonance occurs for $\Omega_2 = \omega_2 - \omega_{ig} = 0$ and is the single-photon $g \to i$ resonance.

To calculate the two-photon line shape and line strength which is obtained in a vapor we must account for atomic motion. For an atom having a z component of velocity, v, the applied optical frequencies are Doppler shifted and are given by $\omega_1(v) = \omega_1(1 - \epsilon v/c)$ and $\omega_2(v) = \omega_2(1 - v/c)$. Use of these frequencies in Eq. (2.4) makes the transition rate Γ velocity dependent. By integrating $\Gamma(v)$ over the Maxwellian thermal velocity distribution we obtain the total two-photon transition rate,

$$\frac{dn}{dt} = \frac{n_0}{\tau_f}\,\frac{|\beta_1|^2\,|\beta_2|^2}{\Delta\nu_i^2\,\Delta\nu_f^2}\,g(a,b), \tag{2.5}$$

where

$$g(a,b) = \frac{y_i^2 y_f^2}{\pi^{9/2}}\int_{-\infty}^{\infty}\frac{e^{-x^2}\,dx}{[(a-x)^2 + y_i^2][(b-x)^2 + y_f^2]}. \tag{2.6}$$

In these equations n_0 is the atomic vapor density, and the other parameters are defined as follows:

$$y_i = (\ln 2)^{1/2} \frac{\Delta\nu_i}{\nu_2 \bar{v}/c}, \tag{2.7}$$

$$y_f = (\ln 2)^{1/2} \frac{\Delta\nu_f}{(\nu_2 + \epsilon\nu_1)\bar{v}/c}, \tag{2.8}$$

$$a = 2(\ln 2)^{1/2} \frac{\nu_2 - \nu_{ig}}{\nu_2 \bar{v}/c}, \tag{2.9}$$

$$b = 2(\ln 2)^{1/2} \frac{\nu_1 + \nu_2 - \nu_{fg}}{(\nu_2 + \epsilon\nu_1)\bar{v}/c}, \tag{2.10}$$

$$\bar{v} = (8kT \ln 2/m)^{1/2}. \tag{2.11}$$

For the purposes of the following discussion it is quite accurate to substitute ν_{ig} for ν_2 and ν_{fi} for ν_1 in the denominators of Eqs. (2.7)–(2.10). Thus y_i is proportional to the natural linewidth of the intermediate state normalized by the Doppler broadening of the $g \to i$ transition; similarly, y_f is proportional to the natural linewidth of the excited state f normalized by the Doppler broadening (full or residual) of the two-photon $g \to f$ transition. The parameter a measures the mistuning of ν_2 from the single-photon $g \to i$ resonance normalized to the $g \to i$ Doppler width; the parameter b measures the mistuning from the two-photon $g \to f$ resonance normalized to the two-photon Doppler width.

At this point let us consider the evaluation of $\mathcal{G}$ in two limiting situations. We will make use of the fact that for low-pressure atomic systems we have $y_i \ll 1$. First we consider the off-resonance situation for which $a \gg 1$. The main contribution to $\mathcal{G}$ comes from the region $-3 \leq x \leq 3$, and the denominator containing a in Eq. (2.6) varies little over this range. Consequently, the denominator can be taken outside the integral and we obtain

$$\mathcal{G} = (y_i^2 y_f/\pi^{7/2} a^2)\, \mathrm{Re}\, w(b + iy_f), \tag{2.12}$$

where $w(z)$ is the error function for complex arguments.[11] This solution is essentially the same as that derived previously for the off-resonance case.[8,12] The line is centered at $b = 0$, which corresponds to the two-photon resonance condition

$$\nu_1 + \nu_2 = \nu_{fg}. \tag{2.13a}$$

The line shape has the form of a Voigt profile, that of a Gaussian convolved with a Lorentzian, and for the case $y_f \ll 1$ its linewidth (FWHM) is approximately given by

$$(\bar{v}/c)(\nu_2 + \epsilon\nu_1), \tag{2.13b}$$

the Doppler width of the two-photon transition.

For the other limiting case, $a \ll 1$, the main contribution to $\mathcal{G}$ comes from the region $|x| \ll 1$. Thus the factor e^{-x^2} may be replaced by unity and the integral becomes the convolution of two Lorentzian functions, which is itself Lorentzian. In this limit we find

$$\mathcal{G} = \frac{y_i y_f (y_i + y_f)}{2\pi^{9/2}} \frac{1}{(b-a)^2 + (y_i + y_f)^2}. \tag{2.14}$$

The line is a Lorentzian centered at $b = a$, which corresponds to

$$\nu_1 + \nu_2 - \nu_{fg} = [(\nu_2 + \epsilon\nu_1)/\nu_2](\nu_2 - \nu_{ig}), \tag{2.15a}$$

and has a Doppler-free linewidth (FWHM) of

$$\Delta\nu_f + (|\nu_2 + \epsilon\nu_1|/\nu_2)\Delta\nu_i. \tag{2.15b}$$

Since we have assumed an infinite lifetime for the ground state (for instance, we neglected transit-time broadening), there is no ground-state contribution to this linewidth. More complete expressions for the linewidth can be found in the work cited in Ref. 4.

For arbitrary values of the mistuning parameter a the generalized two-photon spectrum is composed of both types of lines. For $a \ll 1$ the narrow, Doppler-free line given by Eq. (2.14) predominates. For $a \gg 1$ the Doppler-broadened line given by Eq. (2.12) is the strongest. However, for $a \sim 1$, the two lines are of comparable strength and both contribute to the two-photon line shape.

To obtain the general solution we note that the integral $\mathcal{G}$ [Eq. (2.6)] can be expressed in closed form in terms of $w(z)$, the error function for complex argument[11]:

$$w(a + iy) = \frac{1}{\pi} \int_{-\infty}^{\infty} \frac{[y + i(a-x)]\, e^{-x^2}}{(a-x)^2 + y^2}\, dx. \tag{2.16}$$

The denominator of the integrand of $\mathcal{G}$ can be expanded in partial fractions as

$$\frac{1}{[(a-x)^2 + y_i^2][(b-x)^2 + y_f^2]} = \frac{c_1 + c_2(a-x)}{[(a-x)^2 + y_i^2]} + \frac{c_3 + c_4(b-x)}{[(b-x)^2 + y_f^2]}, \tag{2.17}$$

where the coefficients c_k are given by the following equations:

$$\begin{aligned} \alpha_i &\equiv c_1 - iy_i c_2 = [(b - a - iy_i)^2 + y_f^2]^{-1}, \\ \alpha_f &\equiv c_3 - iy_f c_4 = [(a - b - iy_f)^2 + y_i^2]^{-1}. \end{aligned} \tag{2.18}$$

Equations (2.6) and (2.16)–(2.18) can then be combined to obtain the desired result for $\mathcal{G}$,

$$\mathcal{G} = (y_i y_f/\pi^{7/2})\mathrm{Re}[\, y_f \alpha_i w(a + iy_i) + y_i \alpha_f w(b + iy_f)]. \tag{2.19}$$

This equation gives the generalized two-photon line shape.

We now discuss several qualitative features of $\mathcal{G}(a, b)$. In Fig. 2 we display graphs of $\mathcal{G}(a, b)$ as a

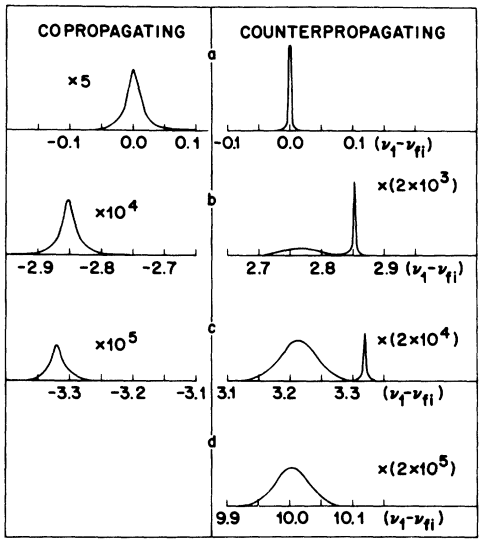

FIG. 2. Two-photon line shape for copropagating and counterpropagating laser beams as a function of $\nu_1-\nu_{fi}$ (in GHz). The parameters used in calculating these curves are given in the text. The four cases (a), (b), (c), and (d) correspond to values for the parameter a (or $\nu_2-\nu_{ig}$ in GHz) of 0 (0), −2.315 (−2.75), −2.694 (−3.2), and −8.418 (−10.0), respectively. Magnification factors for the vertical scales are shown for each case.

function of $\nu_1-\nu_{fi}$ for various values of the parameter a. The two-photon line shapes are plotted for both $\epsilon=+1$ and -1. We emphasize that the plots are for the simple three-level atom shown in Fig. 2. In general, the multilevel character of real atomic states must be taken into account, as will be done in Sec. III, where we compare experiment with theory. In this section we rely on the three-level model to illuminate the qualitative features.

The parameters used in plotting Fig. 2 are typical of those for $3S\rightarrow 4D$ two-photon transitions in sodium vapor using the $3P_{1/2}$ level as the intermediate state. They are $\nu_2=c/(5896\ \text{Å})=5.088\times10^{14}$ Hz, $\nu_1=c/(5682\ \text{Å})=5.280\times10^{14}$ Hz, $\Delta\nu_i=10.0$ MHz, and $\Delta\nu_f=3.1$ MHz. Assuming a vapor temperature of 200°C ($\bar{v}=9.71\times10^4$ cm/sec), we have $y_i=4.2\times10^{-3}$ and $y_f=6.4\times10^{-4}$ for $\epsilon=+1$ or $y_f=-3.46\times10^{-2}$ for $\epsilon=-1$. The on-resonance case is shown in Fig. 2(a), and it is clear that only the Doppler-free line is of importance. As a (proportional to $\nu_2-\nu_{ig}$) is increased, the narrow lines for the $\epsilon=+1$ and -1 cases move in opposite directions. Also, the amplitude of the Doppler-free line falls more rapidly than that of the Doppler-broadened line, and at $a\approx1$ the contribution of both lines is apparent. Because the Doppler-broadened copropagating line is so wide (3.5 GHz FWHM), it does not appear in Fig. 2. For large a, the Doppler-broadened lines predominate. Roughly speaking, for $a\gg1$ the broad lines fall off as a^{-2}, whereas the narrow lines fall off approximately as $\exp(-a^2)$. Note also that in Fig. 2 the peak of the Doppler-broadened line does not occur exactly at $\nu_2+\nu_1=\nu_{fg}$ ($b=0$). This "frequency pulling" has not previously been discussed and could be of importance in applications in which the absolute two-photon resonant frequency ν_{fg} must be accurately determined.

The origin of the frequency pulling is most easily illuminated for the case $a\gg1$. The line peak shifts because the actual line shape is somewhat distorted from the solution given by Eq. (2.12). This distortion occurs because the denominator $(a-x)^2+y_i^2$ in Eq. (2.6) is not actually constant over $|x|\leq3$. A first-order calculation of the frequency pulling is carried out by expanding the denominator to first order in x instead of replacing it by a^2. If this is done it is easy to show that for $a\gg1$ the peak of $\mathcal{I}(a,b)$ occurs at $b=1/a$. Written in terms of frequencies, we find that the peak of the line occurs for

$$\nu_2+\nu_1-\nu_{fg}\approx\frac{1}{4\ln2}\,\frac{[(\nu_2+\epsilon\nu_1)\bar{v}/c]\,\nu_2\bar{v}/c}{\nu_2-\nu_{ig}}\,. \quad (2.20)$$

Using the parameters given above for the near-resonance case, this equation yields a frequency pulling given by $3.70\times10^{16}/(\nu_2-\nu_{ig})$ Hz for oppositely propagating beams. Note that for the case of equal-frequency photons propagating in opposite directions Eq. (2.20) predicts no frequency pulling.

In Sec. III we experimentally verify most of the calculated predictions of this section.

III. EXPERIMENTAL

Our experimental setup was similar to that which we utilized in earlier work.[3,13] A schematic diagram of the basic layout is shown in Fig. 3. Light from two single-axial-mode cw dye lasers operating at different wavelengths (~589 and ~569 nm) propagated in the same or opposite directions through a 1-cm-long Pyrex cell containing atomic sodium vapor at a pressure of about 10^{-5} Torr. Both laser beams were low intensity, having beam diameters of about 2 cm. Two-photon transitions from the $3S$ ground state of sodium to the $4D$ excited state were detected by using a 1P28 photomultiplier to detect the fluorescence at 330 nm ($4P$-$3S$ transition) which results when atoms decay from the $4D$ levels. Either the $3P_{1/2}$ or the $3P_{3/2}$ level could be used as the dominant intermediate state. Two Corning CS7-54 glass filters were used before the photomultiplier to reject scattered laser light and sodium resonance fluorescence while passing light at 330 nm. The main body of the sodium cell was contained in a transparent oven and maintained at a temperature of about 200 °C; the sodium density was determined

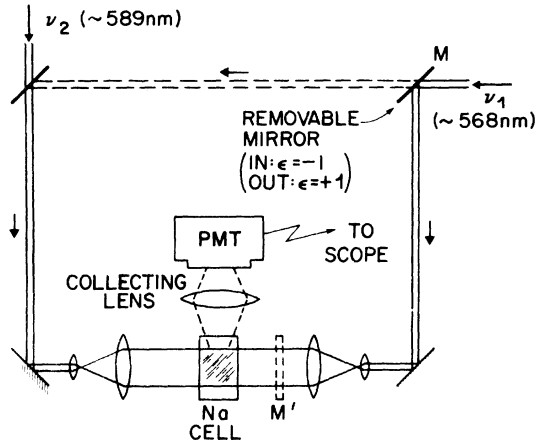

FIG. 3. Schematic diagram of the experimental setup. The laser beams at the frequencies ν_1 and ν_2 are obtained from two single-mode cw dye lasers. The partially transmitting mirror M′ was usually not present.

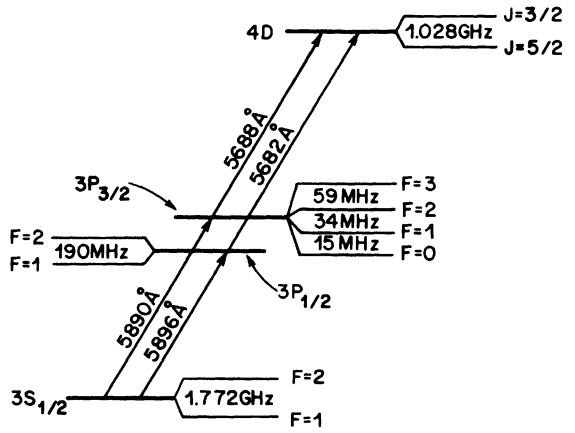

FIG. 4. Various energy levels of atomic sodium (including fine and hyperfine structure) which are important for our experiments.

by the temperature of a sidearm which contained metallic sodium. The density was kept low enough so that even when the 589-nm laser was tuned to be resonant with the $3S$-$3P$ transition the cell illumination was fairly uniform over its length.

The two-photon spectra were recorded by keeping the frequency ν_2 of the 589-nm laser constant while the frequency ν_1 of the 568-nm laser was electronically swept through the various two-photon resonances. Since the frequency ν_2 was nearly resonant with the $3S$-$3P$ transition the two-photon signals were large and could be displayed directly on an oscilloscope. The horizontal axis of the oscilloscope was driven by the frequency sweep electronics of the ν_1 laser, so that the horizontal deflection was proportional to changes in ν_1. With repetitive sweeping of the ν_1 laser through the two-photon resonances, the oscilloscope display was a steady picture of the two-photon spectrum. At slow sweep speeds and with a high-resolution display the frequency jitter of our two lasers (~12 MHz each) became a problem. This situation could be greatly alleviated by increasing the sweep speed to near its maximum (4 GHz scan in 10^{-2} sec). In this case the effect of laser jitter during a single sweep was nearly eliminated, although sweep-to-sweep irregularity was still present. Thus our high-resolution data were obtained by photographing a single-sweep display.

In analyzing the observed two-photon spectra it is necessary to account for the fact that sodium is not a simple three-level atom. The various levels of atomic sodium which are important for our experiments are shown in Fig. 4, along with their fine and hyperfine structures. This multiplicity of levels makes it more difficult to evaluate the two-photon transition rate. We emphasize that Eqs. (2.5) and (2.6) cannot be directly applied to the solution. Instead, it is necessary to go back and to correctly account for all of the atomic levels in calculating $a_f^{(2)}$. When this is done, Eq. (2.4) for Γ may be rewritten to explicitly display the sum over states as

$$\Gamma = \frac{1}{\tau_f} \sum_g \sum_f \left| \sum_i \frac{e^{-i(\omega_1+\omega_2-\omega_{fg})t}}{-i(\omega_1+\omega_2-\omega_{fg})+1/2\tau_f} \times \frac{\beta_1(f,i)\beta_2(i,g)}{i\Omega_2(i,g)-1/2\tau_i} \right|^2 . \tag{3.1}$$

The sum is over all of the intermediate-state sublevels i which connect the various degenerate final-state sublevels f with the degenerate ground-state sublevels g being considered.

To obtain the line-shape function, we follow the procedure used in Sec. II to account for the Doppler shift, and integrate $\Gamma(v)$ over the Maxwellian velocity distribution. The final result is obtained in a straightforward manner and it consists of a sum of error functions of complex arguments. In comparing theory with experiment we have numerically evaluated this complete solution using the sodium level structure shown in Fig. 4 and the relevant experimental parameters. The important point here is that the qualitative features (linewidth, etc.) of the spectra which were enumerated in Sec. II remain the same. When the lasers are tuned far from the intermediate-state resonance, the two-photon spectrum consists of several Doppler-broadened lines, the number and splittings of which are determined by the ground- and final-state structures. The on-resonance case is slightly more complicated. As described in Sec. I, the ν_2 beam has the effect of selecting that velocity group which is resonant with a ground-to-inter-

mediate-state transition. If the ground state has structure, a different velocity group will be selected by a beam at fixed ν_2 for each possible ground-to-intermediate-state transition. Hence when ν_1 is swept, two-photon resonances occur for each different velocity group. The difference in the Doppler shifts of the velocity groups causes a ground-state splitting $\delta\nu_g$ to appear in the spectrum as a splitting of $(\nu_1/\nu_2)\delta\nu_g$, as can be readily verified from Eq. (2.15a). Similarly, structure in the intermediate state will give rise to a splitting in the spectrum of $\delta\nu_i(\nu_2+\epsilon\nu_1)/\nu_2$. For counter-propagating beams and $\nu_2 \sim \nu_1$ the resultant lines tend to merge together. For copropagating beams the splitting is much larger and the on-resonance two-photon spectrum can yield Doppler-free information about the intermediate-state level structure. It is interesting to note that since the linewidth of the two-photon spectrum for oppositely propagating beams is $\Delta\nu_f + |(\nu_2-\nu_1)/\nu_2|\Delta\nu_i$, this linewidth is fairly insensitive to $\Delta\nu_i$. In particular, we can infer that it is only *slightly* dependent upon power broadening of the intermediate state. This fact was experimentally verified.

A typical spectrum obtained using copropagating beams is shown in Fig. 5(a) for ν_2 tuned onto resonance with the $3S_{1/2}$-$3P_{1/2}$ transition (λ_2 = 5895.9 Å). The four lines observed correspond to the four possible transitions from the two hyperfine levels of the ground state to the $4D_{3/2}$ excited state via each of the two hyperfine levels of the $3P_{1/2}$ intermediate state. The splitting between lines a and c and between lines b and d is equal to $\nu_1/\nu_2 = 1.038$ times the hyperfine splitting of the $3S$ ground state. The splitting between lines a and b and between lines c and d is $(\nu_2+\nu_1)/\nu_2 = 2.038$ times the hyperfine splitting of the $3P_{1/2}$ level. The observed splittings are consistent with calculated values. In Fig. 5(b) the lines a and b are shown on an expanded frequency scale; the additional lines a' and b' (which are unresolved and appear as a single line) are the spectral lines corresponding to lines a and b but which are obtained with oppositely propagating beams. Both types of spectra were simultaneously recorded by inserting mirror M′ in Fig. 3 (mirror M, of course, is not present). The frequency ν_2 was adjusted such that lines a' and b' fell between lines a and b. From Eq. (2.15a) the calculated splitting between lines a' and b' is 7.2 MHz. While not apparent on this picture, the lines a' and b' were barely resolved on even further expanded frequency scales, as shown in Fig. 5(c). The linewidth calculated from Eq. (2.15b) for lines a and b is 23.6 MHz; using the frequency splitting as a calibration, the observed linewidth is 30 MHz. For lines a' and b' the calculated linewidth is 3.6 MHz; accounting for the splitting between lines a' and b', we deduce an experimental linewidth of 9.1 MHz. The differences between the calculated and observed linewidths are most probably due to pressure broadening which arises from collisions between sodium atoms and a background gas. The vapor cell used in this work was a sealed unit, and from previous experience we know that background pressures on the order of 0.1–1.0 Torr are to be expected due to outgasing during tipoff. Only several tenths of a Torr of background gas are needed to account for the amount of broadening we observed.[14] To first order these collision effects can be accounted for in our calculations by letting $\Delta\nu_i$ and $\Delta\nu_f$ be the collision-broadened homogeneous linewidths of the respective levels. That is, $2\pi\Delta\nu = 1/\tau_N + 1/\tau_c$, where τ_N is the natural lifetime of the level and τ_c is the mean time between collisions.

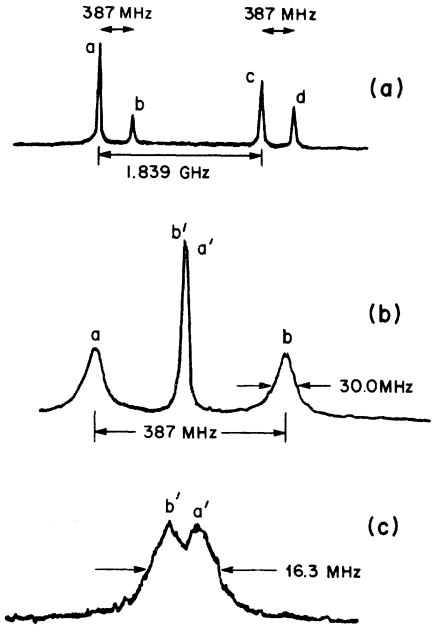

FIG. 5. Typical two-photon spectra obtained with ν_2 tuned onto resonance with the $3S_{1/2} \rightarrow 3P_{1/2}$ transition in sodium vapor. The frequencey ν_1 is scanned through the two-photon resonances and the horizontal scale in these figures is proportional to changes in ν_1. The three cases are described in detail in the text.

In Figs. 6 and 7 we present a detailed comparison of the experimental line shape with theory. The two-photon transitions were from the $3S_{1/2}(F=2)$ ground state to the $4D_{3/2}$ excited state, the $3P_{1/2}$ level was used as the intermediate state, and the data were taken with oppositely propagating beams (mirror M is in and mirror M′ is out in Fig. 3). The frequency ν_2 was adjusted so that both Doppler-free and Doppler-broadened lines were important. We specify the frequency ν_2 with reference to ν_0, the frequency of the $3S_{1/2}(F=2)$-

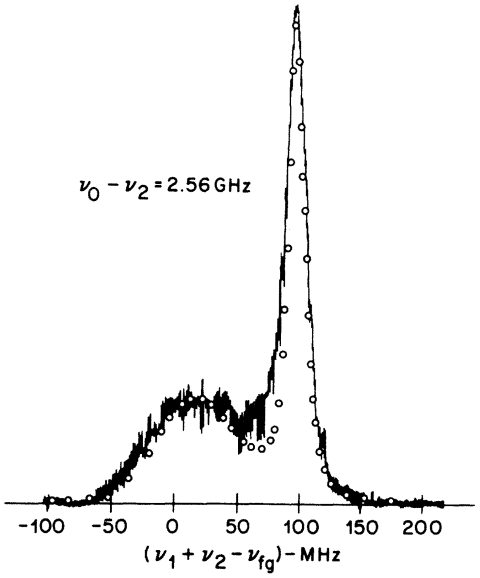

FIG. 6. Comparison of the experimental two-photon line shape obtained using oppositely propagating beams with theory (open circles). The frequency ν_2 was fixed at $\nu_0 - \nu_2 = 2.56$ GHz and the frequency ν_1 was scanned through the two-photon resonance. Other details are given in the text.

$3P_{1/2}(F=1)$ transition. The method we used to measure the detuning will be explained later in this section. We could determine $\nu_2 - \nu_0$ to better than 50 MHz. In our calculations we assumed that the $3P$ and $4D$ levels were equally broadened by collisions and we found that best agreement between theory and experiment was obtained using $1/2\pi\tau_c = 6$ MHz; this amount of broadening could be accounted for by 0.2 Torr of neon. For Fig. 6 the mistuning was $\nu_2 - \nu_0 = -2.56$ GHz, with corresponding values of a, for the two intermediate states, of -2.15 and -2.31; for Fig. 7 the mistuning was -2.75 GHz and the values of a were -2.31 and -2.47. Once again, the narrow peak

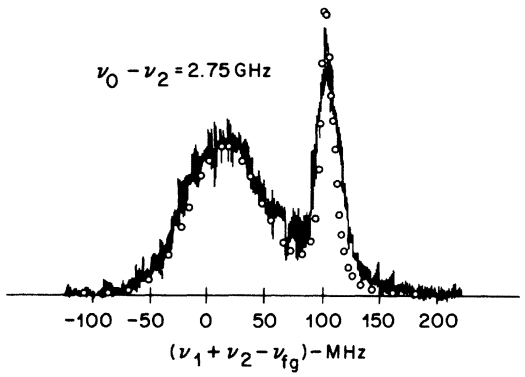

FIG. 7. Same as Fig. 6, but with the frequency ν_2 fixed at $\nu_0 - \nu_2 = 2.75$ GHz.

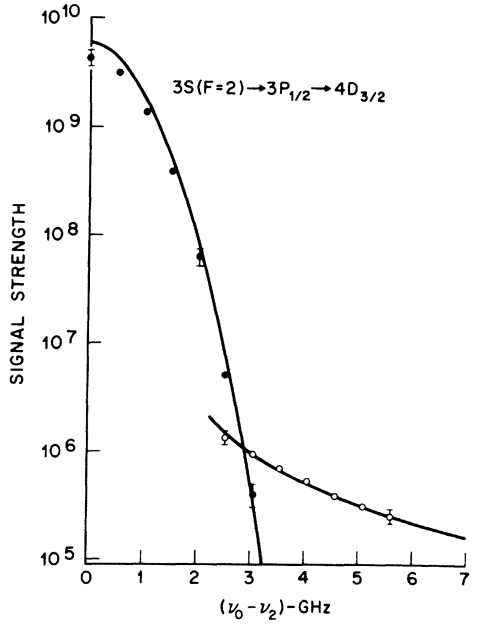

FIG. 8. Experimentally measured and theoretically calculated peak heights for oppositely propagating beams as a function of the detuning, $\nu_0 - \nu_2$. The solid circles (and corresponding curve) are for the Doppler-free on-resonance line. The open circles (and corresponding curve) are for the Doppler-broadened off-resonance line.

is actually composed of two lines which are not resolved. The agreement between theory and experiment is excellent. These data and Fig. 5(c) show that the resolution achieved in our experiments is limited by the slight amount of pressure broadening.

In Fig. 8 we plot the experimentally measured and theoretically calculated peak heights as a function of the detuning $\nu_2 - \nu_0$ for the same situation as in Figs. 6 and 7. The rapid increase of the strength of the narrow Doppler-free line with decreases of $|\nu_2 - \nu_0|$ is readily apparent. The overall agreement between experiment and theory is quite pleasing. In the region $|\nu_2 - \nu_0| < 2$ GHz, the observed line strengths for the Doppler-free line are somewhat less than predicted. We believe this discrepancy is due to the strong single-photon absorption of the ν_2 beam in this region, which results in a falloff of intensity over the length of the vapor cell. The vertical scale in Fig. 8 was chosen so that unity corresponds to the signal strength for equal-frequency beams. The on-resonance line strength is 6×10^9 larger. The behavior of the Doppler-broadened line for large mistunings was experimentally determined in Ref. 3.

In Fig. 9 we present the calculated frequency pulling of the off-resonance Doppler-broadened line as a function of $\nu_2 - \nu_0$. The data are plotted for the $3S(F=2)$-$4D_{3/2}$ two-photon transition using

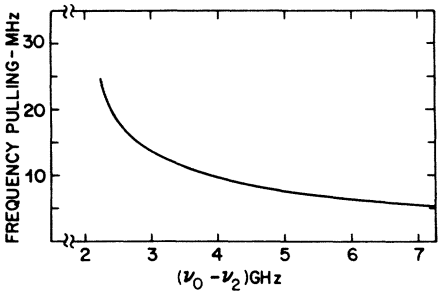

FIG. 9. Calculated frequency pulling of the off-resonance Doppler-broadened line as a function of $\nu_0 - \nu_2$ when the $3P_{1/2}$ level is used as the intermediate state and the laser beams are counterpropagating.

the $3P_{1/2}$ level as the intermediate state and using oppositely propagating laser beams. While the calculated shifts of the line may be significant from the standpoint of frequency standards, they were too small for us to measure.

In Fig. 10 we used copropagating beams to probe the structure of the $3P_{3/2}$ state by observing the $3S_{1/2}(F=2) \rightarrow 4D_{5/2}$ two-photon transition [Fig. 10(a)] and the $3S_{1/2}(F=1) \rightarrow 4D_{5/2}$ transition [Fig. 10(b)]. The $F=3$, 2, and 1 hyperfine levels of the $3P_{3/2}$ state are the intermediate states in Fig. 10(a), while the $F=2, 1$, and 0 hyperfine levels are the intermediate states in Fig. 10(b). The resolution we observe compares favorably with the best resolution previously obtained using other techniques. The splittings observed yield hyperfine

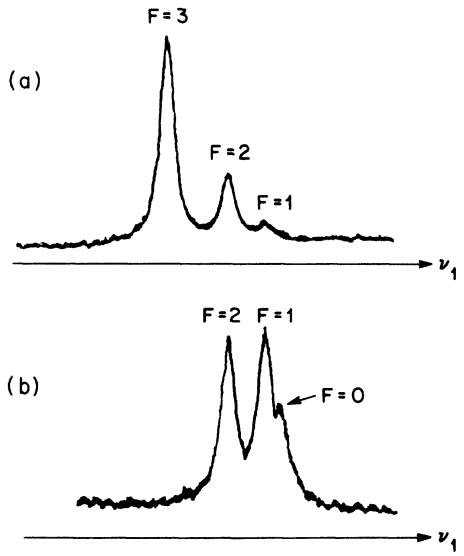

FIG. 10. Hyperfine structure of the $3P_{3/2}$ state of atomic sodium observed using two-photon absorption with copropagating beams and the $3P_{3/2}$ level as a resonant intermediate state. In (a) ν_2 is tuned such that the $3S_{1/2}(F=2) \rightarrow 4D_{5/2}$ transition is observed; in (b) the $3S_{1/2}(F=1) \rightarrow 4D_{5/2}$ transition is used.

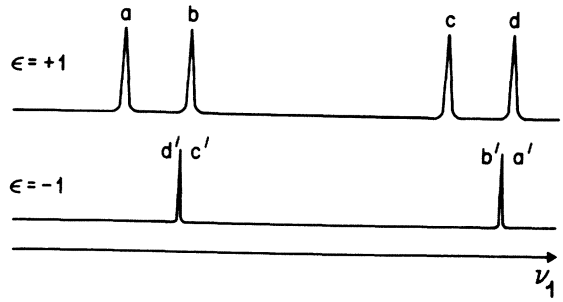

FIG. 11. Schematic diagram of the on-resonance $3S_{1/2} \rightarrow 4D_{3/2}$ two-photon spectrum observed with copropagating ($\epsilon = +1$) and oppositely propagating ($\epsilon = -1$) beams and using the $3P_{1/2}$ level as the intermediate state. As explained in the text, by observing the relative positions of the $\epsilon = +1$ and -1 spectra, ν_2 can be accurately tuned to the various $3S_{1/2} \rightarrow 3P_{1/2}$ resonances.

intervals between the $F=3$ and $F=2$ levels, between the $F=2$ and $F=1$ levels, and between $F=1$ and $F=0$ levels of 60, 34, and 14 MHz, respectively, in good agreement with previous values[15] of 59, 34, and 15 MHz. The broad background signal apparent in Fig. 10 is due to excitation of the $3P_{3/2}$ level by trapped resonance fluorescence which is omnidirectional; the background is easily eliminated by reducing the vapor density.

The final subject we wish to discuss in this section is a novel method for accurately tuning the ν_2 laser into resonance with the various transitions between the ground-state hyperfine levels and the intermediate-state hyperfine levels. This can be done to an accuracy of better than 10 MHz, even though the Doppler width of these single-photon transitions is about 1.7 GHz. This method is part of the technique used to measure $\nu_2 - \nu_0$, as mentioned earlier. The essence of the technique is to simultaneously observe the two-photon spectrum for copropagating and oppositely propagating beams. An example was shown earlier in Fig. 5(b), with moderate resolution. In Fig. 11 we show the same situation, but at lower resolution. All of the lines which occur for the $3S_{1/2} \rightarrow 3P_{1/2} \rightarrow 4D_{3/2}$ transition are shown. As the frequency ν_2 is increased the lines for $\epsilon = +1$ move to the right-hand side (higher ν_1) in Fig. 11 and the lines for $\epsilon = -1$ move to the left-hand side. If ν_2 is tuned such that lines d and d', c' overlap, then ν_2 is tuned onto resonance with the $3S(F=2) \rightarrow 3P(F=1)$ transition ($\nu_2 = \nu_0$). Different values for ν_2 were accurately obtained by starting at $\nu_2 = \nu_0$ and then changing ν_2 in increments by hopping over several axial modes of the ν_2 laser (the axial mode spacing was accurately known). Smaller changes in ν_2 were monitored using a scanning Fabry-Perot interferometer. We believe our values for $\nu_2 - \nu_0$ were accurate to better than 50 MHz. The other

$3S_{1/2} \rightarrow 3P_{1/2}$ transition frequencies were also easily obtained. For instance, overlapping lines c and d', c' means ν_2 is tuned to the $3S(F=2) \rightarrow 3P_{1/2}(F=2)$ transition; overlapping lines b and b', a' corresponds to the $3S(F=1) \rightarrow 3P_{1/2}(F=1)$ transition; and overlapping lines a and b', a' corresponds to the $3S(F=1) \rightarrow 3P_{1/2}(F=2)$ transition.

IV. CONCLUSION

In this paper we have theoretically and experimentally investigated the line shape and strength of two-photon absorption in an atomic vapor using a resonant, or nearly resonant, intermediate state. It was shown that the spectrum was characterized by two types of lines. The first type is characteristic of the far–off-resonance case and it exhibits Doppler broadening. Except for the small frequency-pulling effects, which are discussed here for the first time, the properties of this line has been previously discussed.[8] The second type of line predominates for the resonant, or nearly resonant, case and is free of Doppler broadening. The two-photon transition rates are maximized and the Doppler-free lines are obtained with either copropagating or oppositely-propagating laser beams. The on-resonance lines are related to spectra obtained using laser-induced line-narrowing techniques.[4] The on-resonance lines obtained with oppositely propagating beams are quite insensitive to power broadening of the intermediate state. A disadvantage with the on-resonance situation is that absolute two-photon transition frequencies are not easily obtained, since the two-photon resonance sum frequency differs from ν_{fg} unless $\nu_2 = \nu_{ig}$. Nonetheless, the technique is a good one for determining level intervals. Since signal strengths are maximized, the on-resonance case should be useful for carrying out two-photon spectroscopy of particularly weak two-photon transitions.[16] By simultaneously observing the spectra caused by both copropagating and oppositely propagating beams, the ν_2 laser can be accurately tuned to the transitions between the various hyperfine levels of the ground and intermediate states.

An additional feature of on-resonance two-photon spectroscopy is that Doppler-free spectra of the intermediate state can be obtained in a vapor, with a resolution which rivals the best obtained using single-photon absorption and well-collimated atomic beams. Our experimental observations are in excellent agreement with theoretical calculations. By frequency scanning one laser at a rapid rate we are able to greatly reduce the effects of laser frequency jitter and to obtain real-time two-photon spectra with a resolution limited by pressure broadening to about 7 MHz.

ACKNOWLEDGMENT

The authors thank Dr. S. Stenholm for discussions which stimulated our interest in this problem.

[1]L. S. Vasilenko, V. P. Chebotaev, and A. V. Shishaev, Zh. Eksp. Teor. Fiz. Pis'ma Red. 12, 161 (1970) [JETP Lett. 12, 113 (1970)]; F. Biraben, B. Cagnac, and G. Grynberg, Phys. Rev. Lett. 32, 643 (1974); M. D. Levenson and N. Bloembergen, Phys. Rev. Lett. 32, 645 (1974); T. W. Hänsch, K. C. Harvey, G. Meisel, and A. L. Schawlow, Opt. Commun. 11, 50 (1974). For a summary of more recent work see B. Cagnac, in *Laser Spectroscopy: Proceedings of the Second International Conference, Megève, June 23-27, 1975*, edited by S. Haroche *et al.* (Springer, Berlin, 1975), p. 165.

[2]W. K. Bischel, P. J. Kelly, and C. K. Rhodes, Phys. Rev. Lett. 34, 300 (1975).

[3]J. E. Bjorkholm and P. F. Liao, Phys. Rev. Lett. 33, 128 (1974).

[4]For example, see M. S. Feld and A. Javan, Phys. Rev. 177, 540 (1969); T. Hänsch and P. Toschek, Z. Phys. 236, 213 (1970); I. M. Beterov and V. P. Chebotaev, in *Progress in Quantum Electronics*, edited by J. H. Sanders and S. Stenholm (Pergamon, New York, 1974), Vol. 3, Pt. 1.

[5]These facts are explicitly, but qualitatively, pointed out in Ref. 10 of H. T. Duong, S. Liberman, J. Pinard, and J. L. Vialle, Phys. Rev. Lett. 33, 339 (1974).

[6]R. Salomaa and S. Stenholm, J. Phys. B 8, 1795 (1975).

[7]We have recently learned of calculations which include detailed collision effects, carried out by P. R. Berman, Phys. Rev. A 13, 2191 (1976).

[8]J. E. Bjorkholm and P. F. Liao, IEEE J. Quantum Electron. QE-10, 906 (1974).

[9]H. K. Holt, Phys. Rev. Lett. 19, 1275 (1967).

[10]C. Delsart and J. C. Keller, Opt. Commun. 15, 91 (1975).

[11]W. Gautschi, in *Handbook of Mathematical Functions*, edited by M. Abramowitz and I. A. Stegun (Natl. Bur. Stand., U.S. GPO, Washington, D. C., 1965), p. 297.

[12]In Ref. 8 we incorrectly used $\Delta\nu = 1/\pi\tau$, instead of the correct expression $\Delta\nu = 1/2\pi\tau$, as the relationship between the natural linewidth and natural lifetime of an atomic energy level.

[13]P. F. Liao and J. E. Bjorkholm, Phys. Rev. Lett. 34, 1 (1975).

[14]F. Biraben, B. Cagnac, and G. Grynberg, J. Phys. (Paris) Lett. 36, 41 (1975). See also W. Shütz, Z. Phys. 45, 30 (1927).

[15]H. T. Duong *et al.*, Opt. Commun. 7, 371 (1973).

[16]P. F. Liao and J. E. Bjorkholm have observed on-resonance $3S \rightarrow 4F$ two-photon transitions in sodium vapor. The $3P \rightarrow 4F$ coupling occurs via an electric quadrupole matrix element [Phys. Rev. Lett. 36, 1543 (1976)].